

# A Multiplex Technology Platform for the Rapid Analysis of Clinically Actionable Genetic Alterations and Validation for *BRAF* p.V600E Detection in 1549 Cytologic and Histologic Specimens

David L. Smith, PhD; Aude Lamy, PhD; Sylvie Beaudenon-Huibregtse, PhD; Richard Sesboué, MD; Walairat Laosinchai-Wolf, PhD; Jean-Christophe Sabourin, PhD, MD; Emmanuel Labourier, PhD

• **Context.**—Current clinicopathologic assessment of malignant neoplastic diseases entails the analysis of specific genetic alterations that provide diagnostic, prognostic, or therapy-determining information.

**Objective.**—To develop and validate a robust molecular method to detect clinically relevant mutations in various tissue types and anatomic pathology specimens.

**Design.**—Genes of interest were amplified by multiplex polymerase chain reaction and sequence variants identified by liquid bead array cytometry. The *BRAF* assay was fully characterized by using plasmids and genomic DNA extracted from cell lines, metastatic colorectal cancer formalin-fixed, paraffin-embedded (FFPE) tissues, and thyroid nodule fine-needle aspirates.

**Results.**—Qualitative multiplex assays for 22 different mutations in the *BRAF*, *HRAS*, *KRAS*, *NRAS*, or *EGFR* genes were established. The high signal-to-noise ratio of the technology enabled reproducible detection of *BRAF*

c.1799T>A (p.V600E) at 0.5% mutant allele in 20 ng of genomic DNA. Precision studies with multiple operators and instruments showed very high repeatability and reproducibility with 100% (98.7%–100%) qualitative agreement among 292 individual measures in 38 runs. Evaluation of 1549 representative pathologic specimens in 2 laboratories relative to independent reference methods resulted in 99.0% (97.6%–99.6%) agreement for colorectal FFPE tissues (n = 416) and 98.9% (98.2%–99.4%) for thyroid fine-needle aspiration specimens (n = 1133) with an overall diagnostic odds ratio of 10 856 (2451–48 078).

**Conclusions.**—The multiplex assay system is a sensitive and reliable method to detect *BRAF* c.1799T>A mutation in colorectal and thyroid lesions. This optimized technology platform is suitable for the rapid analysis of clinically actionable genetic alterations in cytologic and histologic specimens.

(*Arch Pathol Lab Med*. doi: 10.5858/arpa.2013-0002-OA)

With the advent of personalized medicine, molecular testing plays a growing role in clinical oncology and clinical pathology practices. In many cases, the analysis of specific genetic alterations complements the cytopathologic or histopathologic evaluation of solid tumor specimens and provides additional valuable information to ascertain diagnosis or predict outcome and select optimal therapeutic options. For example, treatment of non-small cell lung cancer with tyrosine kinase inhibitors targeting the epider-

mal growth factor receptor (EGFR) requires previous knowledge of mutations associated with drug sensitivity or resistance.<sup>1</sup> In metastatic colorectal cancer (mCRC), the use of anti-EGFR monoclonal antibodies is restricted to patients with tumors wild type for *KRAS* in codons 12 and 13.<sup>2,3</sup> Other mutations in genes downstream of the EGFR signaling pathway, such as *BRAF* codon 600, are further associated with poor outcome and increased mortality in mCRC.<sup>4,5</sup> The mutated and activated *BRAF* kinase (p.V600E) is also a druggable target and a specific inhibitor is now approved in Europe and the United States for use in first-line treatment of patients with metastatic melanoma.<sup>6,7</sup> In thyroid cancer, testing for *BRAF*, *KRAS*, *HRAS*, and *NRAS* mutations, as well as chromosomal rearrangements involving the *RET* or *PAX8* proto-oncogenes, increasingly contributes to the optimal surgical management of papillary thyroid carcinoma.<sup>8,9</sup>

Several technologies attuned to the clinical laboratory workflow and instrumentation have been developed over the years to achieve sensitive and specific detection of various clinically actionable genetic alterations. Most of these assays rely on end-point polymerase chain reaction (PCR) followed by Sanger sequencing, pyrosequencing, or amplicon detection by sizing or probe-hybridization tech-

Accepted for publication May 17, 2013.

From Asuragen Inc, Austin, Texas, (Drs Smith, Beaudenon-Huibregtse, Laosinchai-Wolf, and Labourier); the Department of Pathology, Rouen University Hospital, Rouen, France (Drs Lamy and Sabourin); and INSERM U1079, Faculty of Medicine, Rouen University, Rouen, France (Dr Sesboué).

Drs Smith, Beaudenon-Huibregtse, Laosinchai-Wolf, and Labourier are employees of Asuragen Inc, Austin, Texas. The other authors have no relevant financial interest in the products or companies described in this article.

Supplemental digital content is available for this article at [www.archivesofpathology.org](http://www.archivesofpathology.org).

Reprints: Emmanuel Labourier, PhD, Asuragen Inc, 2150 Woodward St, Suite 100, Austin, TX 78744 (e-mail: [elabourier@asuragen.com](mailto:elabourier@asuragen.com)).

niques.<sup>10,11</sup> Another common method is to perform simultaneous amplification and fluorescence detection by using real-time PCR instruments and a variety of chemistries such as intercalating dyes, hydrolysis probes, or self-probing amplicons.<sup>12–14</sup> Because the multiplexing capability and throughput of these technologies are somewhat limited, alternative methods capable of detecting several mutations from distinct genes have also been developed. For example, multiplex primer extension reactions followed by capillary electrophoresis sizing (SNaPshot, Life Technologies, Carlsbad, California) have been successfully implemented in the clinical setting.<sup>15,16</sup> Likewise, solution hybridization of multiple PCR products on addressable microspheres, followed by flow cytometry fluorescence analysis, is broadly used in clinical diagnostic applications for bacterial, viral, genetic, or oncology targets.<sup>17–21</sup>

Regardless of the technology platform, molecular methods currently in clinical use have been optimized to be compatible with anatomic pathology specimens. Because of the breadth of specimen types and preanalytic parameters commonly encountered in the clinical setting, the quantity or quality of nucleic acids recovered from these specimens can vary greatly. For the preoperative molecular assessment of papillary thyroid carcinoma, specimens are in general fine-needle aspirates (FNAs) from suspicious nodules with an indeterminate cytologic diagnosis.<sup>8,9</sup> Depending on the cellularity and conditions of collection, storage, and extraction, the yield or integrity of the resulting purified genomic DNA (gDNA) can be severely compromised. For colorectal cancer, mutational analysis is performed on postsurgical formalin-fixed, paraffin-embedded (FFPE) tissues after histologic diagnosis.<sup>2,3,10–12</sup> The quality of gDNA extracted from these specimens can be dramatically affected by intramolecular and intermolecular cross-links and chemical modifications resulting in DNA fragmentation and sequence alteration.<sup>15,22</sup>

Preliminary studies have shown that distinct *KRAS* mutations can be detected by multiplex PCR and liquid bead array flow cytometry.<sup>17</sup> The goals of the present study were to expand the technology to relevant genetic alterations in *BRAF* and other genes in the *EGFR* pathway, to perform a complete analytic validation of the assay system, and to evaluate its performance with a large number of representative cytopathologic and histopathologic specimens.

## MATERIALS AND METHODS

### Clinical Specimens

All human specimens in this study were residual, deidentified gDNA samples for research purpose. No results were reported to physicians or patients or used for treatment decision and no protected health information or other information identifying patients was released. At both study sites, 10- to 20- $\mu$ m-thick sections from FFPE mCRC specimens were macrodissected to selectively exclude nonmalignant, stromal, and contaminating inflammatory cells and obtain a minimum of 40% tumor content. Genomic DNA was then extracted from the tumor-enriched specimens by using laboratory-developed methods based on the RecoverAll Total Nucleic Acid Isolation Kit for FFPE Tissues (Life Technologies, Carlsbad, California) at both sites. Genomic DNA from thyroid nodules was prepared at site 2 by using a laboratory-developed method based on the *mirVana* PARIS Kit (Life Technologies) and single-pass FNAs collected and stored in *RNAretain*, a single-use vial containing a nontoxic solution for the preservation and stabilization of intracellular nucleic acids

(Asuragen, Austin, Texas). All human gDNA samples were quantified by using a GeneQuant *pro* (GE Healthcare Biosciences, Pittsburg, Pennsylvania) at site 1 or a NanoDrop ND1000 (NanoDrop Technologies, Waltham, Massachusetts) at site 2.

### Plasmids, Cell Lines, and Dilution Samples

Plasmid DNA carrying specific mutations were prepared at site 2 by using the QIAprep Spin Miniprep Kit (Qiagen, Hilden, Germany) and characterized by bidirectional sequencing with the Sanger method. Genomic DNA from fresh cultured cell lines was prepared at site 2 by using the QIAamp DNA Mini Kit (Qiagen), and the presence of specific genetic alterations was verified by Sanger sequencing. The following amino acid changes were confirmed: *BRAF* p.V600E (HT29), *EGFR* p.L858R/p.T790M (H1975), *EGFR* p.E746\_A750del (H1650), *EGFR* p.T790M/p.E746\_A750del (H820), *KRAS* p.G12A (SW1116), *KRAS* p.G12D (PL45), *KRAS* p.G12V (SW480), *KRAS* p.G13D (HCT116), *HRAS* p.G12V (T24), *NRAS* p.Q61K (HT1080), and *NRAS* p.Q61R (SKMEL2). Samples for analytic characterization experiments were prepared at site 2 by serial dilution based on the nucleic acid concentration as determined by NanoDrop ND1000 (NanoDrop Technologies) for each sample. Samples positive for a given mutation (plasmid, cell line, thyroid FNA, or mCRC FFPE) were diluted in a background of purified gDNA from a cell line confirmed negative for that specific mutation, keeping the total concentration of gDNA constant. Allele copy numbers in gDNA samples were estimated by using a rounded value of 3.3 pg for the mass of a haploid human genome, corresponding to about 300 allele copies per ng of gDNA.

### Molecular Assays

DNA specimens were tested with the Signature *BRAF* Mutations Kit (for research use only; Asuragen) or prototype assays, following the protocol described in Laosinchai-Wolf et al.<sup>17</sup> Briefly, DNA samples were first amplified by multiplex PCR using gene-specific biotin-modified primers. Biotinylated amplified products were then directly hybridized to mutation-specific capture probes covalently conjugated to carboxylated microspheres. Following addition of fluorescent reporter, the probe-bound PCR products were detected by flow cytometry on a Luminex 200 system (Luminex, Austin, Texas). Fluorescence signals were calculated by using a minimum of 50 beads for each target. Primers and probe sequences were according to the Catalog of Somatic Mutations in Cancer Web site ([www.sanger.ac.uk/genetics/CGP/cosmic](http://www.sanger.ac.uk/genetics/CGP/cosmic), accessed November 16, 2012). Polymerase chain reaction amplifications and hybridization reactions were performed on a GeneAmp PCR System 9700 or a Veriti 96-Well Thermal Cycler (Life Technologies). The reference method at site 1 was the PCR/SNaPshot assay described in Lamy et al.<sup>15</sup> Amplifications were performed by using 100 to 1000 ng of gDNA and followed by primer extension reactions using sense or antisense SNaPshot primers and the ABI PRISM SNaPshot Multiplex Kit (Life Technologies). The purified labeled products were resolved on an ABI PRISM 3130xl Genetic Analyzer (Life Technologies) and analyzed by using GeneMapper Software version 4.0 (Life Technologies). The reference method at site 2 was a laboratory-developed real-time PCR assay using the primers and hydrolysis probes described in Smyth et al.<sup>23</sup> Amplifications were performed with 10 ng of gDNA on a 7500 Real-Time PCR System (Life Technologies).

### Data Analysis

Percentage agreements were calculated by using qualitative assay results (positive or negative) before discrepancy analysis. Quantitative analyses of signals were performed in Excel 2010 (Microsoft Corp, Redmond, Washington). Analysis of the positive and negative signal distributions at site 1 was performed by using the retest results for the 3 samples initially discrepant. Limit of blank (LOB) values were calculated according to current guidelines (mean plus 1.645 times the standard deviation), assuming 1-sided normal-like distribution of negative signals.<sup>24</sup> Confidence intervals

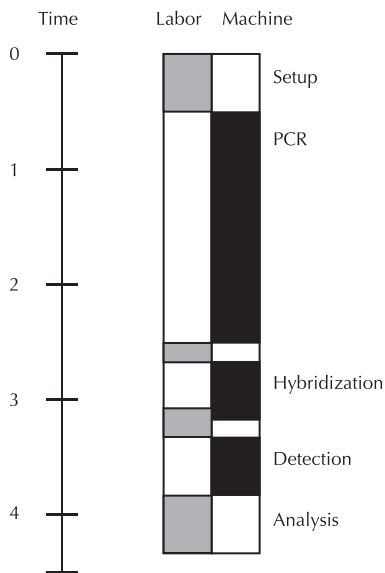


**Figure 1.** Assay workflow and time-motion analysis. The graphic shows the steps and time requirements to perform 48 reactions (1 kit equivalent) in a 96-well plate. The grey and black boxes represent the operator and instrument times (in hours), respectively. Abbreviation: PCR, polymerase chain reaction.

were calculated by using the Wilson score interval for percentage agreements or the method described by Armitage and Berry for diagnostic odds ratios.<sup>25–27</sup>

## RESULTS

### Assay Workflow

The qualitative assay system consisted of 3 steps: (1) multiplex PCR amplification on purified gDNA, (2) hybridization of PCR products onto probes conjugated to spectrally distinct beads, and (3) simultaneous bead sorting and fluorescence analysis by flow cytometry (Figure 1). For 48 reactions in a 96-well plate format, the total assay time was less than 4 hours with approximately 1 hour of labor time and 3 hours of instrument time. The subsequent data analysis step was straightforward with qualitative interpretation of the median fluorescence intensity (MFI) signals reported for each target-specific bead population relative to a single positive/negative cutoff value (500 MFI). Representative examples of assay output, including amplification and detection of an endogenous control sequence and 3 plate/run controls, are presented in Table 1.

### Qualitative Analysis of Distinct Gene Mutations

Evaluation of the *BRAF* assay with 20 ng of gDNA extracted from well-characterized cell lines or 6000 copies of plasmids spiked into 20 ng of gDNA from the *BRAF* mutation-negative cell line DU145 showed specific detection of the mutation c.1799T>A (p.V600E) with a high signal-to-noise ratio (Table 1). With the same multiplex technology and workflow, mutational analysis of *BRAF* codon 600 was effectively combined with the detection of 12 distinct mutations in *KRAS* codons 12 and 13 (Supplemental Tables 1 through 3; [supplemental digital content](#)). No cross-detection was observed between *BRAF* and 7 *KRAS* mutations in codons 12/13 or 5 additional rare mutations in *KRAS* codon 13. Similarly, 6 distinct mutations in *HRAS*

**Table 1. Representative Examples of Median Fluorescence Intensity Signal With the *BRAF* Assay**

	c.1799T>A	EC
Negative control	62	<b>7168</b>
Positive control	<b>10 952</b>	<b>7822</b>
No DNA control	78	76
DU145 cell line gDNA	115	<b>10 490</b>
PL45 cell line gDNA	91	<b>10 110</b>
HT29 cell line gDNA	<b>13 457</b>	<b>10 488</b>
HCT116 cell line gDNA	121	<b>10 533</b>
SW1116 cell line gDNA	182	<b>10 860</b>
<i>BRAF</i> c.1799T>A plasmid	<b>15 137</b>	<b>10 858</b>
<i>BRAF</i> wild-type plasmid	166	<b>10 513</b>

Abbreviations: EC, endogenous control; gDNA, genomic DNA.

Values in bold indicate positive signals above the qualitative cutoff.

codons 12/61 or *NRAS* codon 61 could be detected in a single-well assay (Supplemental Table 4; see supplemental digital content at [www.archivesofpathology.org](http://www.archivesofpathology.org)). In addition to single-nucleotide substitutions, other types of genetic abnormalities, such as deletions in *EGFR* exon 19, could be assessed in the same reaction (Supplemental Table 5; see supplemental digital content at [www.archivesofpathology.org](http://www.archivesofpathology.org)). The presence of multiple genetic alterations in a given test sample, for example *EGFR* p.T790M plus p.L858R or p.T790M plus p.E746\_A750del, did not interfere with the assay. Overall, multiplex assays for 22 relevant mutations in the *BRAF*, *HRAS*, *KRAS*, *NRAS*, or *EGFR* genes were successfully established (Table 2). To fully characterize the technology platform, extensive validation studies were next performed with the prototypic *BRAF* assay.

### Normal Range and LOB

The range of MFI signals in well-characterized, true negative samples was determined by repetitively testing 5 sample types (Table 3). A no-DNA template control and a plasmid DNA containing no *BRAF*-related sequences were tested in triplicate in 15 runs and *BRAF*-negative cell line, thyroid nodule FNAs, and mCRC FFPE tissue samples were tested in triplicate in 9 runs. The distributions of negative signals generated by the *BRAF* c.1799T>A probe across 171 independent measures were similar in the absence or presence of gDNA (Table 3). Analysis at the sample level also showed similar performance for different sample types (Figure 2). Mean signals (73 to 88 MFI), standard deviations (35 to 47 MFI), and maximum signals (170 to 259 MFI) were all in the same range. The calculated LOB values, representing 95% of the signal distribution for each sample type, were at least 3-fold lower than the 500 MFI cutoff value ( $3 \times \text{LOB} = 421$  to  $492$  MFI and  $447$  MFI overall; Figure 2). These data indicate that a false-positive qualitative result (c.1799T>A probe signal  $>500$  MFI) is not expected in true negative samples ( $P < .001$ ).

### Analytic Sensitivity and Specificity

To confirm the analytic specificity of the *BRAF* assay and determine its limit of detection (LOD) relative to the 500 MFI cutoff, serial dilutions of gDNA extracted from c.1799T>A-positive cultured cell line (HT29), thyroid nodule FNA, or mCRC FFPE tissue were tested (Figure 3, A). The LOD was between 0.1% and 1% dilution at 20-ng gDNA input for all sample types. Additional mapping experiments suggested a LOD between 0.4% and 0.8% dilution (Supplemental Table 6; see supplemental digital

<i>BRAF</i>	<i>EGFR</i>	<i>HRAS</i>	<i>KRAS</i>	<i>KRAS</i>	<i>NRAS</i>
p.V600E	p.L858R p.T790M DEL19	p.G12V p.Q61K p.Q61R	p.G12A p.G12C p.G12D p.G12R p.G12S p.G12V	p.G13A p.G13C p.G13D p.G13R p.G13S p.G13V	p.Q61K p.Q61L p.Q61R

Abbreviation: DEL19, p.E746\_A750del in exon 19.

	Replicate	Run	Measure	MIN	MAX	Median	Mean	SD
No gDNA (n = 2)	3	15	90	0	259	78	79	39
With gDNA (n = 3)	3	9	81	0	237	82	82	45
Overall	3	24	171	0	259	82	81	42

Abbreviations: gDNA, genomic DNA; MAX, maximum; MIN, minimum.

content at [www.archivesofpathology.org](http://www.archivesofpathology.org)) and repeated testing with independent dilutions of HT29 gDNA showed reproducible detection at 0.5% dilution (Figure 3, B). Coamplification of *BRAF* and *KRAS* in a single reaction format resulted in a minimal decrease in c.1799T>A probe signal and a LOD of 1% (Supplemental Figure 1; see supplemental digital content at [www.archivesofpathology.org](http://www.archivesofpathology.org)). To further investigate analytic specificity, a series of plasmids carrying individual mutations were tested in multiple runs (Supplemental Table 7; see supplemental digital content at [www.archivesofpathology.org](http://www.archivesofpathology.org)). The plasmids c.1799\_1800delinsAT (p.V600D), c.1799\_1800delinsAA (p.V600E2), and c.1798\_1799delinsAA (p.V600K) reproducibly generated MFI signal above the 500 MFI cutoff. No cross-detection was observed with plasmids carrying other mutations affecting *BRAF* codon 600 or surrounding codons, such as single-nucleotide substitutions (p.A598V, p.V600A, or p.K601E), insertions (p.A598\_T599insV), or deletions (p.V600\_K601>E) (Supplemental Table 8; see supplemental digital content at [www.archivesofpathology.org](http://www.archivesofpathology.org)).

### Method Precision

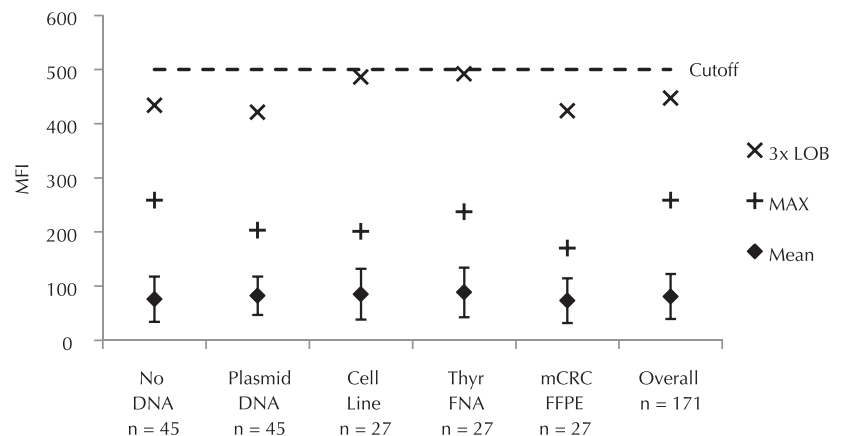
In the analytic experiments described above, all replicates across all runs generated the same qualitative positive/negative results. To fully validate the method precision, 8 additional studies were performed with the *BRAF* assay (Table 4). Within-run precision (repeatability) was evaluated by testing 4 medium to low positive samples (20%, 10%,

4%, and 2% HT29 dilutions) in quadruplicate and 2 low positive samples (2% and 1% HT29 dilutions) in 12 replicates (n = 40). Between-run precision (reproducibility) was evaluated by testing the positive, negative, and no-DNA template controls provided with the kit in 26 runs with 3 different operators (n = 78). Total precision (within-laboratory precision) was further evaluated by testing (1) high, medium, and low positive samples (100%, 20%, and 2% HT29 dilutions) and 1 negative sample (DU145) in triplicate in 5 runs with 3 operators (n = 60), (2) six thyroid nodule FNAs or mCRC FFPE samples (3 positive and 3 negative) in triplicate in 3 runs with the same operator (n = 54), and (3) five thyroid nodule FNAs or mCRC FFPE samples (3 positive and 2 negative) in quadruplicate in 3 runs with 3 operators (n = 60). There was 100% qualitative agreement between all replicates and all runs for a total of 292 individual measures (95% confidence intervals: 98.7%–100%) (Table 4). A precision of 100% (97.9%–100%) was also observed for the hybridization step only by performing 3 independent hybridizations on the same day with 2 instruments and 7 samples amplified in quadruplicate (n = 84) and 4 independent hybridizations on 4 different days on the same instrument with 8 samples amplified in triplicate (n = 96) (Table 4).

### Compatibility With Pathologic Specimens

To assess the multiplex technology with different tissue types, specimen processing methods, and testing sites, the

**Figure 2.** Limit of blank (LOB) studies. The graph shows the mean of the median fluorescence intensity (MFI) signals for the c.1799T>A probe, the maximum (MAX) MFI, and 3 times the calculated LOB value (3× LOB) for each of the 5 samples and overall relative to the qualitative 500 MFI cutoff value (dashed line). The error bars represent the standard deviations of each distribution. Abbreviations: mCRC FFPE, metastatic colorectal cancer formalin-fixed, paraffin-embedded tissue; Thyр FNA, thyroid nodule fine-needle aspirate.



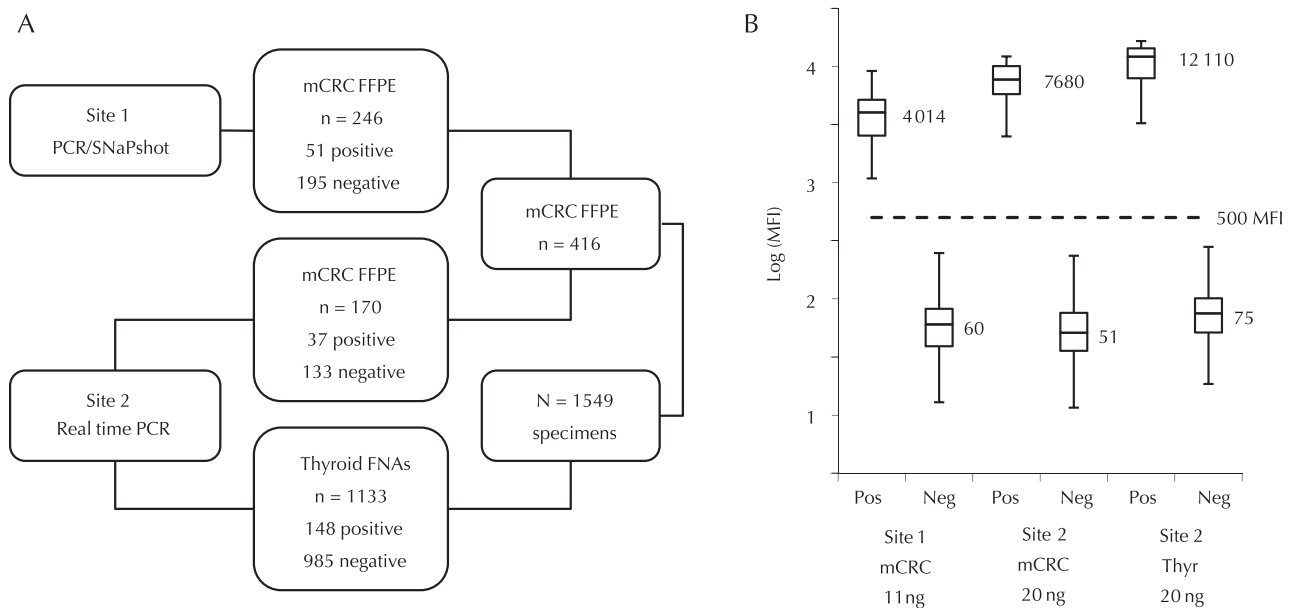
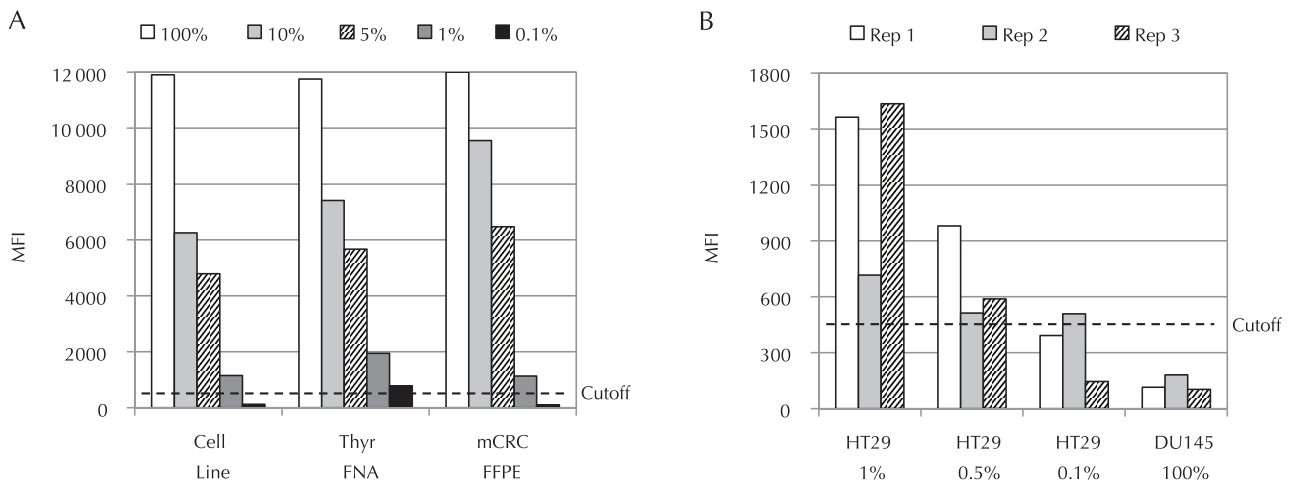


**Figure 3.** Limit of detection studies. *A*, Representative example of median fluorescence intensity (MFI) signals for the *c.1799T>A* probe with genomic DNA (gDNA) extracted from *BRAF* mutation-positive cell line (HT29), thyroid nodule fine-needle aspirate (Thyr FNA), or metastatic colorectal cancer formalin-fixed, paraffin-embedded tissue (mCRC FFPE). The samples were tested undiluted (100%) or diluted at 10%, 5%, or 0.1% positive gDNA in a background of *BRAF* mutation-negative gDNA from the cell line DU145 (20-ng total input). The dashed line represents the qualitative 500 MFI cutoff value. *B*, Representative example of replicate assay results (Rep 1, Rep 2, Rep 3) for the *c.1799T>A* probe with 1%, 0.5%, or 0.1% dilutions of HT29 gDNA and undiluted DU145 gDNA (20-ng total input). The dashed line represents the qualitative 500 MFI cutoff value.

**Figure 4.** Evaluation of representative clinical specimens. *A*, Overview of study design. A total of 1549 residual genomic DNA (gDNA) samples from metastatic colorectal cancer formalin-fixed, paraffin-embedded tissue blocks (mCRC FFPE) or thyroid nodule fine-needle aspirates (thyroid FNAs) were evaluated at 2 sites by using distinct reference methods. PCR/SNaPshot, polymerase chain reaction followed by primer extension using the SNaPshot (Life Technologies, Carlsbad, California) technology. *B*, Quantitative analysis of signal output. The boxes represent the 25th, 50th (median), and 75th percentiles of the positive (Pos) and negative (Neg) *c.1799T>A* probe signal distributions for each site and sample type. The tails of the distributions are indicated by whiskers corresponding to 1.5 times the interquartile range (75th percentile value minus the 25th percentile value) or the maximum/minimum values of the distributions if within the interquartile range. The median fluorescence intensity (MFI) values for each signal distribution and the qualitative 500 MFI cutoff value (dashed line) are also shown. Abbreviation: Thyr, thyroid nodule fine needle aspirate.

*BRAF* assay was next evaluated with a set of 1549 representative cytologic and histologic specimens (Figure 4, A). A total of 416 residual mCRC FFPE gDNA samples were tested retrospectively at 2 sites, one in Europe and one in the United States. The sample set was enriched for known *BRAF c.1799T>A*-positive specimens to obtain a statistically significant number of positive samples ( $n = 88$  or 21.2% of the mCRC samples). The 1133 residual gDNA

samples from thyroid nodule FNAs collected in 26 states across the United States were tested consecutively at 1 site without knowledge of the cytologic or histologic diagnoses. As the set contained a mixture of lesions with benign, suspicious, malignant, or indeterminate cytology, the prevalence for *BRAF c.1799T>A* was 13.1% (148 of 1133). Quantitative analysis of the 1549 *c.1799T>A* probe signals generated with the *BRAF* assay during the study showed a

Precision	PCR and Hybridization						Hybridization Only	
	Within-Run		Between-Run	Total (Within-Laboratory)			Within-Day	Between-Day
Run	1	1	26	5	3	3	3	4
Sample	4	2	3	4	6	5	7	8
Replicate	4	12	1	3	3	4	4	3
Measure	16	24	78	60	54	60	84	96
Operator	1	1	3	3	1	3	1	1
Instrument	1	1	2	2	1	1	2	1
Agreement, %	100	100	100	100	100	100	100	100

Abbreviation: PCR, polymerase chain reaction.

similar distribution of negative signals across samples and sites (Figure 4, B). The median positive signals were consistent with the differences in specimen types and gDNA inputs (11.25 ng at site 1; 20 ng at site 2). Overall, 95% of the positive signals were at least 3-fold above the cutoff (>1533 MFI) and 95% of the negative signals were at least 3-fold below the cutoff (<159 MFI). These data confirmed the high signal-to-noise ratio of the technology regardless of the potential preanalytic differences between sites or sample types.

#### Agreement With Reference Methods

The qualitative positive/negative *BRAF* assay results were also compared against independent molecular data obtained with reference methods based on multiplex PCR/SNaPshot technology at site 1 or real-time quantitative PCR technology at site 2 (Table 5). For mCRC FFPE specimens, the overall agreement between methods was 99.0% (412 of 416). Testing at site 1 initially resulted in 2 false-negative results with c.1799T>A signals just below the cutoff (431 and 344 MFI) and 1 false-positive result with a low mutant signal (744 MFI). The 3 discrepancies were resolved after retesting (data not shown). At site 2, one apparent false-positive result was observed (1193 MFI) and could not be ruled out after retesting. For thyroid nodule FNA specimens, the overall agreement between methods was 98.9% (1121 of 1133) (Table 5). Twelve apparent false positives were observed and were all confirmed positive after retesting (data not shown). Overall, the positive and negative agreements for the combined 1549 specimens were 99.2% (234 of 236) and 98.9% (1299 of 1313), respectively, with a corresponding diagnostic odds ratio of 10 856 (Table 5).

#### COMMENT

Molecular methods designed to complement the cytopathologic or histopathologic evaluation of solid tumor lesions should be compatible with anatomic pathology specimens. In the present study, the *BRAF* assay was validated relative to established reference molecular methods<sup>15,23</sup> by using 1549 residual gDNA samples extracted from representative thyroid nodule FNAs or mCRC FFPE tissues. The positive, negative, and overall agreements were all greater than 97.7% with lower bound confidence intervals greater than 92.1% in both the cytologic and histologic sample sets. The 12 apparent false-positive results observed with thyroid nodule FNA samples likely reflected the difference in analytic sensitivity between the 2 assays at site 2 (0.5% for the *BRAF* assay, approximately 5% for the reference method). Retesting of these samples and more than 90% of the true-positive samples for which enough residual gDNA was available (n = 134) ruled out a potential technical error or cross-contamination issue. Overall, calculation of the diagnostic odds ratio for the combined 1549 specimens showed an excellent assay performance with a lower bound confidence interval greater than 2451. This metric is a single global indicator of assay performance and measures the effectiveness of a test to predict a disease independently of its prevalence.<sup>27</sup> In our study, it can further be interpreted as the odds of a true-positive *BRAF* assay result (234 of 2) being 10 856 times higher than the odds of a false-positive result (14 of 1299).

For routine use in clinical pathology laboratories, novel molecular methods should also be compatible with the clinical laboratory workflow and demonstrate robust and reliable performance. Comprehensive analytic characteriza-

	<i>BRAF</i> Assay					
	mCRC			Thyroid		
	Pos	Neg	Total	Pos	Neg	Total
Reference methods						
Pos	86	2	<b>88</b>	148	0	<b>148</b>
Neg	2	326	<b>328</b>	12	973	<b>985</b>
<b>Total</b>	<b>88</b>	<b>328</b>	<b>416</b>	<b>160</b>	<b>973</b>	<b>1133</b>
Positive agreement, % (range)	97.7 (92.1–99.4)			100 (97.5–100)		
Negative agreement, % (range)	99.4 (97.8–99.8)			98.8 (97.9–99.3)		
Overall agreement, % (range)	99.0 (97.6–99.6)			98.9 (98.2–99.4)		
Combined agreement, % (range)	99.0 (98.3–99.4)			98.9 (98.2–99.4)		
Combined odds ratio	10 856 (2451–48 078)					

Abbreviations: mCRC, metastatic colorectal cancer; Neg, negative; Pos, positive. Values in parentheses represent the 95% confidence intervals.

tion studies showed reproducible detection of *BRAF* c.1799T>A with different sample types, thermocyclers, flow cytometers, and operators. Both within-run and between run experiments for a total of 38 runs (1 repeatability run and 1 reproducibility run were confounded) resulted in 100% qualitative agreement. Other studies, such as DNA input range (5 to 20 ng recommended), interference by potential residual protein or RNA contaminants, and reagents' or PCR products' stability, further confirmed the *BRAF* assay robustness (data not shown). The LOD was 0.5% dilution, corresponding to 0.1-ng positive gDNA in a background of 20-ng negative gDNA or approximately 15 copies of mutant allele detected in a background of 6000 wild-type alleles (the cell line HT29 is heterozygote for *BRAF* c.1799T>A). Although a lower LOD may be desirable to protect from potential false-negative results, comparative validation studies for such an assay would be extremely challenging owing to the lack of accepted reference methods reaching this level of sensitivity. For example, independent studies have shown that 10% to 20% of mCRC FFPE samples positive by molecular methods with an LOD of approximately 1% were negative by the less sensitive Sanger sequencing method.<sup>12,17,28</sup>

Specificity for the *BRAF* mutation c.1799T>A was confirmed with cell lines and residual clinical specimens, and potentially interfering mutations were evaluated with synthetic plasmids. The observed cross-detection with plasmids c.1799\_1800delinsAT (p.V600D), c.1799\_1800delinsAA (p.V600E2), and c.1798\_1799delinsAA (p.V600K) was not surprising since these double-nucleotide substitutions result in a T to A change at position 1799 such as for p.V600E (c.1799T>A). Previous studies<sup>13,29</sup> have shown that p.V600D, E2, and K can also be sporadically detected by real-time PCR assays designed to detect *BRAF* p.V600E in melanoma specimens. These double mutations are relatively frequent in melanoma but could not be evaluated with representative clinical specimens in our study owing to their scarcity in colorectal and thyroid lesions. Specificity for distinct genes or distinct amplified regions within the same gene was however confirmed with the prototype *BRAF/KRAS, HRAS/NRAS, and EGFR* assays. Our results indicate that a single technology platform can be used for the qualitative analysis of mutations in *BRAF* codon 600, *HRAS* codons 12/61, *KRAS* codons 12/13, *NRAS* codon 61, or *EGFR* codons 790/858, as well as deletions in *EGFR* exon 19. Each assay was performed in less than 4.5 hours in a 96-well plate format with a very favorable signal-to-noise ratio, enabling a simple and safe data interpretation relative to a single qualitative cutoff. Evaluation of serial dilutions with plasmid and cell line samples further suggested a similar LOD of at least 1% or 60 copies of mutant allele for *HRAS, KRAS, NRAS, and EGFR* (data not shown).

Multiplex assay systems provide obvious operational advantages relative to repeated series of individual PCR. In principle, all 22 mutations evaluated here could be further combined in a single assay. However, such a large panel would be extremely difficult to validate for every mutation and pathologic specimen type. Subpanels focusing on specific genes may be more practical, address most clinical needs for different tissue/specimen types, and prevent unnecessary testing. In addition, one advantage of the Luminex flow cytometer is the possibility to simultaneously analyze the fluorescence output from different assays using the multibatch mode. For example, the *KRAS* and *BRAF* assays can be performed in the same run to

assess up to 45 mCRC FFPE specimens in a single 96-well plate, and up to 30 thyroid FNA specimens can be tested for *BRAF, KRAS, and NRAS/HRAS* in a single plate without significantly affecting the workflow or total assay time (data not shown).

Testing for oncogenic gene rearrangements in cytologic thyroid specimens also plays a key role in the management of patients with thyroid cancer to guide appropriate surgical therapy.<sup>8,9</sup> Independently from the present work, the multiplex assay system has been further optimized to detect fusion transcripts resulting from chromosomal inversions or translocations such as *RET-PTC* and *PAX8-PPARG* in thyroid nodule FNA specimens (unpublished results). In addition, preliminary studies suggest that the assays are compatible with histologic FFPE thyroid specimens as well as melanoma, lymph node, and lung tissues (unpublished results). We conclude that the multiplex assay system described here is a general technology platform suitable for the rapid analysis of relevant and clinically actionable genetic alterations in a variety of solid tumor specimens. Future validation studies for specific panels could provide additional speed and flexibility to clinical pathology laboratories and further advance the personalized molecular management of cancer patients.

The authors wish to thank Lauren Friar, BS, Andrew Hadd, PhD, Jeffrey Houghton, MS, Julie Krosting, MS, Maura Lloyd, MS, Rupali Shinde, MS, and Fei Ye, PhD, all from Asuragen Inc, for their technical expertise and contribution during the development of the multiplex assay system.

## References

- West H, Lilenbaum R, Harpole D, Wozniak A, Sequist L. Molecular analysis-based treatment strategies for the management of non-small cell lung cancer. *J Thorac Oncol.* 2009;4(9):S1029-S1039.
- Monzon FA, Ogino S, Hammond ME, Halling KC, Bloom KJ, Nikiforova MN. The role of *KRAS* mutation testing in the management of patients with metastatic colorectal cancer. *Arch Pathol Lab Med.* 2009;133(10):1600-1606.
- Wang HL, Lopategui J, Amin MB, Patterson SD. *KRAS* mutation testing in human cancers: the pathologist's role in the era of personalized medicine. *Adv Anat Pathol.* 2010;17(1):23-32.
- Safaei Ardekani G, Jafarnejad SM, Tan L, Saeedi A, Li G. The prognostic value of *BRAF* mutation in colorectal cancer and melanoma: a systematic review and meta-analysis. *PLoS One.* 2012;7(10):e47054.
- Van Cutsem E, Kohne CH, Lang I, et al. Cetuximab plus irinotecan, fluorouracil, and leucovorin as first-line treatment for metastatic colorectal cancer: updated analysis of overall survival according to tumor *KRAS* and *BRAF* mutation status. *J Clin Oncol.* 2011;29(15):2011-2019.
- Chapman PB, Hauschild A, Robert C, et al. Improved survival with vemurafenib in melanoma with *BRAF* V600E mutation. *N Engl J Med.* 2011;364(26):2507-2516.
- Bollag G, Tsai J, Zhang J, et al. Vemurafenib: the first drug approved for *BRAF*-mutant cancer. *Nat Rev Drug Discov.* 2012;11(11):873-886.
- Mehta V, Nikiforov YE, Ferris RL. Use of molecular biomarkers in FNA specimens to personalize treatment for thyroid surgery [published online ahead of print September 13, 2012]. *Head Neck.* doi:10.1002/hed.23140.
- Nikiforov YE. Molecular analysis of thyroid tumors. *Mod Pathol.* 2011;24:S34-S43.
- Weichert W, Schewe C, Lehmann A, et al. *KRAS* genotyping of paraffin-embedded colorectal cancer tissue in routine diagnostics: comparison of methods and impact of histology. *J Mol Diagn.* 2010;12(1):35-42.
- Kwon MJ, Lee SE, Kang SY, Choi YL. Frequency of *KRAS, BRAF, and PIK3CA* mutations in advanced colorectal cancers: comparison of peptide nucleic acid-mediated PCR clamping and direct sequencing in formalin-fixed, paraffin-embedded tissue. *Pathol Res Pract.* 2011;207(12):762-768.
- Gonzalez de Castro D, Angulo B, Gomez B, et al. A comparison of three methods for detecting *KRAS* mutations in formalin-fixed colorectal cancer specimens. *Br J Cancer.* 2012;107(2):345-351.
- Halait H, Demartin K, Shah S, et al. Analytical performance of a real-time PCR-based assay for V600 mutations in the *BRAF* gene, used as the companion diagnostic test for the novel *BRAF* inhibitor vemurafenib in metastatic melanoma. *Diagn Mol Pathol.* 2012;21(1):1-8.
- Harbison CT, Horak CE, Ledezne JM, et al. Validation of companion diagnostic for detection of mutations in codons 12 and 13 of the *KRAS* gene in patients with metastatic colorectal cancer: analysis of the NCIC CTG CO.17 trial

[published online ahead of print October 3, 2012]. *Arch Pathol Lab Med*. doi:10.5858/arpa.2012-0367-OA.

15. Lamy A, Blanchard F, Le Pessot F, et al. Metastatic colorectal cancer KRAS genotyping in routine practice: results and pitfalls. *Mod Pathol*. 2011;24(8):1090–1100.
16. Lurkin I, Stoehr R, Hurst CD, et al. Two multiplex assays that simultaneously identify 22 possible mutation sites in the KRAS, BRAF, NRAS and PIK3CA genes. *PLoS One*. 2010;5(1):e8802.
17. Laosinchai-Wolf W, Ye F, Tran V, et al. Sensitive multiplex detection of KRAS codons 12 and 13 mutations in paraffin-embedded tissue specimens. *J Clin Pathol*. 2011;64(1):30–36.
18. Defoort JP, Martin M, Casano B, Prato S, Camilla C, Fert V. Simultaneous detection of multiplex-amplified human immunodeficiency virus type 1 RNA, hepatitis C virus RNA, and hepatitis B virus DNA using a flow cytometer microsphere-based hybridization assay. *J Clin Microbiol*. 2000;38(3):1066–1071.
19. Dunbar SA, Jacobson JW. Application of the luminex LabMAP in rapid screening for mutations in the cystic fibrosis transmembrane conductance regulator gene: a pilot study. *Clin Chem*. 2000;46(9):1498–1500.
20. Ye F, Laosinchai-Wolf W, Labourier E. An optimized technology platform for the rapid multiplex molecular analysis of genetic alterations associated with leukemia. *Cancer Genet*. 2012;205(10):488–500.
21. Ye F, Li MS, Taylor JD, et al. Fluorescent microsphere-based readout technology for multiplexed human single nucleotide polymorphism analysis and bacterial identification. *Hum Mutat*. 2001;17(4):305–316.

22. Quach N, Goodman MF, Shibata D. In vitro mutation artifacts after formalin fixation and error prone translesion synthesis during PCR. *BMC Clin Pathol*. 2004;4(1):1.
23. Smyth P, Finn S, Cahill S, et al. RET/PTC and BRAF act as distinct molecular, time-dependant triggers in a sporadic Irish cohort of papillary thyroid carcinoma. *Int J Surg Pathol*. 2005;13(1):1–8.
24. Armbruster DA, Pry T. Limit of blank, limit of detection and limit of quantitation. *Clin Biochem Rev*. 2008;29:S49–S52.
25. Newcombe RG. Two-sided confidence intervals for the single proportion: comparison of seven methods. *Stat Med*. 1998;17(8):857–872.
26. Armitage P, Berry G. *Statistical Methods in Medical Research*. London, England: Blackwell Scientific Publications; 1994.
27. Glas AS, Lijmer JG, Prins MH, Bossuyt PM. The diagnostic odds ratio: a single indicator of test performance. *J Clin Epidemiol*. 2003;56(11):1129–1135.
28. Franklin WA, Haney J, Sugita M, Bemis L, Jimeno A, Messersmith WA. KRAS mutation: comparison of testing methods and tissue sampling techniques in colon cancer. *J Mol Diagn*. 2010;12(1):43–50.
29. Anderson S, Bloom KJ, Vallera DU, et al. Multisite analytic performance studies of a real-time polymerase chain reaction assay for the detection of BRAF V600E mutations in formalin-fixed, paraffin-embedded tissue specimens of malignant melanoma. *Arch Pathol Lab Med*. 2012;136(11):1385–1391.